
Effects of Asymmetric Photopeak Windows on Flood Field Uniformity and Spatial Resolution of Scintillation Cameras

L. Stephen Graham, Richard L. LaFontaine, and Mark A. Stein

Nuclear Medicine Service, Veteran's Administration Medical Center, Sepulveda; Medical Physics Division, UCLA School of Medicine, Los Angeles, U. S. Naval Hospital, San Diego; and Department of Radiology, Beverly Hills Medical Center, Beverly Hills, California

Pulse height analyzer windows that are set on the high side of the photopeak are known to improve spatial resolution and contrast when used for scintillation camera imaging. Asymmetric windows can be used with some scintillation cameras that have energy correction circuitry. In this study the improvement in spatial resolution and loss of field uniformity for ^{99m}Tc , ^{201}TI , and ^{131}I were measured as a function of window asymmetry (up to 30%, defined relative to the loss of counts as compared to a symmetric window under intrinsic conditions). Flood field uniformity was inversely related to the degree of window asymmetry. With 10 cm of scatter the ^{99m}Tc integral uniformity deteriorated from 7.9% with a symmetric window to 11.5% for a 30% asymmetric window. The corresponding values for ^{201}TI were 9.9 and 10.9%. Even without additional scatter, the values for ^{131}I were 23.0 and 26.5%. Spatial resolution, as measured by the full width at half maximum in 10 cm of scatter improved by only 5% for ^{99m}Tc and 7% for ^{201}TI . However, the full width at tenth maximum increased by as much as 20% for ^{99m}Tc and ^{201}TI . A large percentage of this improvement was attained with small degrees of asymmetry. This study demonstrates that 10% or less asymmetry can provide most of the benefit in spatial resolution and contrast that is to be gained without significant losses in field uniformity and count rate.

J Nucl Med 27:706-713, 1986

Because of the poor energy resolution of scintillation detector systems, the pulse height analyzer windows that are commonly used for imaging include substantial numbers of photons that have been scattered (1-3). This reduces the spatial resolution and contrast of the images produced with these windows (4,5). Although this problem exists for all photon energies emitted by commonly used radionuclides, it becomes more serious as photon energy decreases (6,7). The nature of Compton scattering is such that as photon energy decreases, the scattered photon retains a larger and larger percentage of the original energy (8). When the difference in energy is small there is overlap of the photopeak and the Compton portion of the spectrum. As a result, scattered events are accepted by the pulse height analyzer (PHA) and are included in the image formation process. This problem is compounded by the presence of scatter because the ratio of scatter to primary photons in the photopeak increases with depth of the source in a scatter medium (9-11).

A number of years ago it was proposed that the use of analyzer windows set asymmetrically high on the photopeak could be used to improve spatial resolution and contrast by reducing the number of scattered photons included in the PHA window (12). Because the use of asymmetric windows reduces the number of counts in the image if the total time is held constant, considerable effort was put into selecting the optimum window (3,4,13-17). Necessity dictates that there must be a compromise between the improvement in spatial resolution and contrast and the increase in image noise, unless longer imaging times are used. No single window setting is appropriate for all imaging situations because of the variation in the amount of scatter that is present.

Although asymmetric windows were used for early models of scintillation cameras, subsequent improvements in spatial resolution made them particularly sensitive to PHA window settings (18). Asymmetrically high PHA windows produced images of unacceptable field uniformity. The introduction of special electronic

circuits to correct for variations in the location of the photopeak across the face of the NaI(Tl) crystal in scintillation cameras brought about renewed interest in the reduction of scatter by this technique. Steidly et al. demonstrated that asymmetric windows improved lesion contrast and produced sharper edges for both thallium-201 (^{201}Tl) and technetium-99m ($^{99\text{m}}\text{Tc}$) (19).

Subsequently, Lewellen et al. used a series of disks to study edge sharpness and contrast (20,21). Their work confirmed the results obtained by Steidly et al. The improvement in contrast has also been studied by LaFontaine et al. (22). They used a phantom to study the effect on contrast and found it improved by as much as 32% for $^{99\text{m}}\text{Tc}$ and 39% for ^{201}Tl . More recently, Collier et al. reported the use of asymmetric windows on a series of bone imaging studies (23). Both clinical impression and quantitation of images acquired in a computer confirmed the advantage of using asymmetric windows. Ricciardone et al. found similar results with ^{201}Tl (24).

The purpose of this study was to quantitate the changes in spatial resolution and field uniformity as a function of window asymmetry. These data, together with a study of the improvement in contrast and an observer performance study, should prove useful in determining the instrument settings which will provide maximum benefit in clinical imaging.

MATERIALS AND METHODS

Data were collected for this study with a Picker Dyna-Camera 5C (0.95 cm crystal) interfaced to an ADAC 3300 computer through an O'Neill Enterprises box. The box was used to provide additional choices of image magnification and rotation. For $^{99\text{m}}\text{Tc}$ and ^{201}Tl imaging, a HEX 0.070-in. general purpose collimator was used. When iodine-131 (^{131}I) was imaged, a 0.100-in. HEX array collimator was selected. Field uniformity and spatial resolution measurements were made with five different PHA window positions. Symmetrical, 5, 10, 20, and 30% asymmetric (labeled SYM A05, A10, A20, and A30, respectively). Asymmetry was defined on the basis of count loss with respect to the counting rate observed in a symmetric window under intrinsic conditions. A 20% window was used for all $^{99\text{m}}\text{Tc}$ and ^{131}I measurements; the ^{201}Tl window was 25%.

Prior to each data collection session, the Micro-Z energy and renormalization maps (Stages I and II) were loaded following the protocol provided by the manufacturer (25). Subsequent measurements were made with full correction.

Field Uniformity

Four different measurements of field uniformity were made at each of the five window positions. Intrinsic uniformity was measured with the appropriate radionuclide as a point source at a distance of approximately five crystal diameters. The detector was facing upward and electronic masking was employed to minimize edge-packing effects. Fifteen million counts were collected in each image in a $64 \times 64 \times 16$ bit matrix. Care was taken to keep the count rate below 30k cps.

Three extrinsic flood images representing different scatter conditions were obtained for all window positions. For the first, a liquid-filled flood placed directly in contact with the collimator on the inverted detector was used to generate a 15 million count image. The second image was obtained with 5 cm of lucite inserted between the collimator and the flood and 5 cm of lucite on top of the flood. Conditions for acquiring the third image were similar except that a total of 10 cm of lucite was placed between the collimator and the flood. In all studies, care was taken to thoroughly mix the flood and to keep the sides of the phantom flat.

Field uniformity was quantitated by four different parameters for both the central and useful field-of-view (CFOV and UFOV). The method described by Keyes et al. was used to calculate the percentage of pixels within above, and below the mean with a 2 s.d. allowance for counting statistics (26). Field uniformity was also calculated by the method of Cox and Difley (Uniformity Index, UI) which expresses uniformity as the total variance in the image minus the variance that is associated with counting statistics (27). Finally, the National Electrical Manufacturers Association (NEMA) protocol was used to compute the integral and differential field uniformity (28).

To test the reliability of these measurements, symmetric windows were used on intrinsic $^{99\text{m}}\text{Tc}$ floods and measured independently 19 separate times involving 12 different Micro-Z loadings. Similar but less extensive tests were performed with ^{201}Tl (three independent measurements with three separate Micro-Z loadings).

Spatial Resolution

Three different techniques were used to evaluate changes in spatial resolution as a function of analyzer window position. A NEMA slit pattern and the NEMA protocol were used to measure intrinsic spatial resolution in one central region of the CFOV using a $256 \times 256 \times 16$ bit matrix. To provide adequate data sampling, a zoom factor of 5:1 was used (three-fold factor by computer; 1.7 factor in the O'Neill box). Intrinsic resolution was not measured for ^{131}I because of the excessive penetration of the higher energy photons through the NEMA pattern.

Measurement of extrinsic resolution was made with two different scatter conditions. For one, a 1.0-mm inside diameter line source embedded in lucite 5 cm from the collimator face with 5 cm of back scatter was used. For the second, the line source was 10 cm from the collimator face with 5 cm of back scatter. For each measurement the full width at half maximum (FWHM) and full width at tenth maximum (FWTM) were computed.

RESULTS

Field Uniformity

The results of the field uniformity measurements for $^{99\text{m}}\text{Tc}$ are presented in Fig. 1. It is important to note that when the Keyes et al. method is used, poorer uniformity is associated with a smaller percentage. In contrast, when the NEMA integral, NEMA differential, and Uniformity Index (UI) methods are used, the percentage increases as uniformity deteriorates. Intrinsic field uniformity for $^{99\text{m}}\text{Tc}$ was very insensitive to the degree of asymmetry. By the Keyes et al. method of analysis, field uniformity for the CFOV, defined as the per-

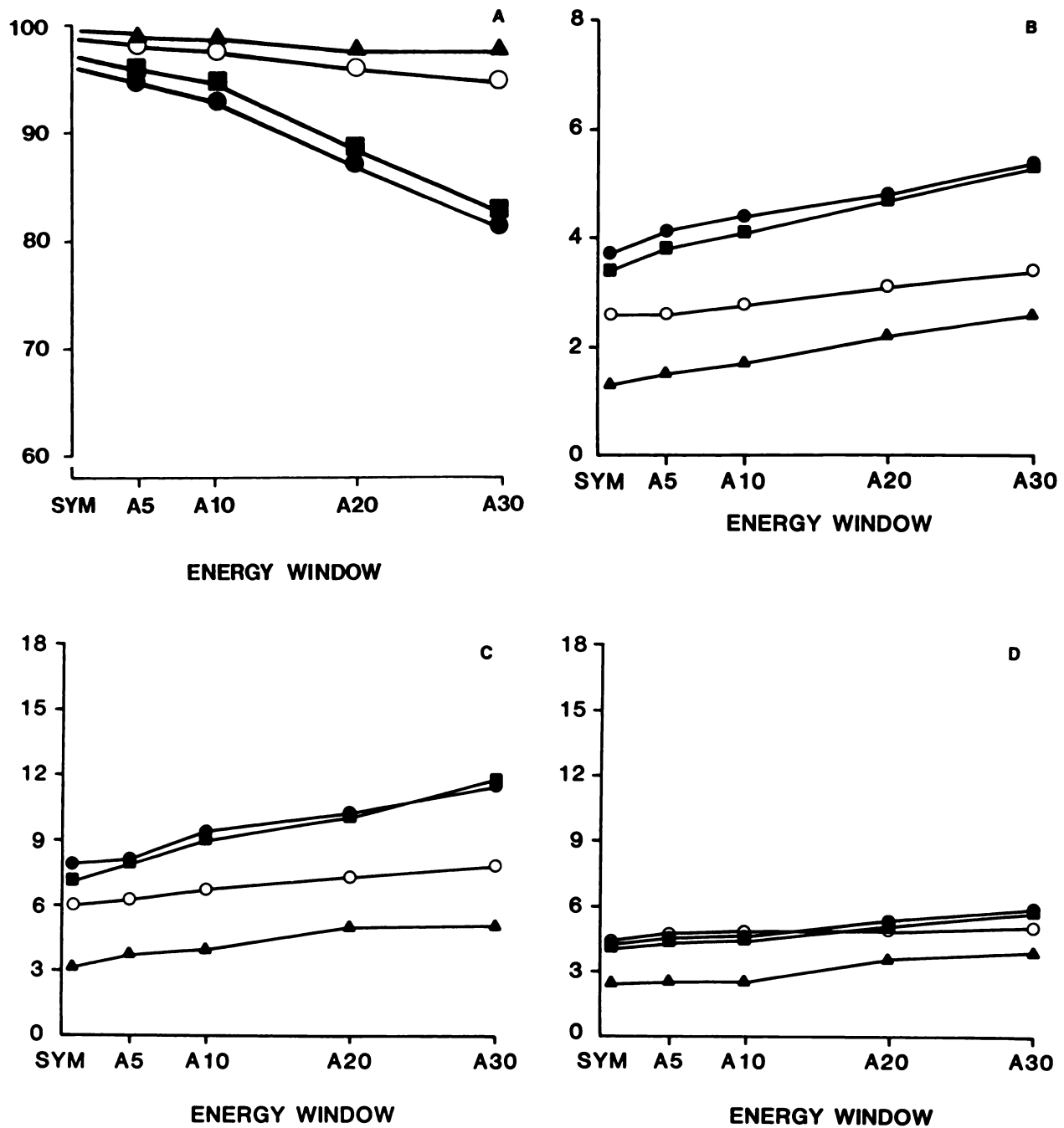


FIGURE 1

A: Technetium-99m flood field uniformity measured by percentage of cells within 5% of the mean (Keyes et al.) as function of analyzer window asymmetry for four different scatter configurations: (▲) Intrinsic; (○) Extrinsic liquid-filled flood; (■) Extrinsic flood with 5 cm scatter and 5 cm backscatter (●) Extrinsic flood with 10 cm scatter and 5 cm backscatter. B: ^{99m}Tc flood field uniformly measured by the UI as function of analyzer window asymmetry for four different scatter configurations. C: ^{99m}Tc integral flood field uniformity measured by NEMA algorithm as function of analyzer window asymmetry for four different scatter configurations. D: ^{99m}Tc differential flood field uniformity measured by NEMA algorithm as a function of analyzer window asymmetry for four different scatter configurations

centage within $\pm 5\%$ of the mean, decreased from 100 to 99.6% when the window was moved from the SYM position to A30, a percentage loss of 0.4, while the NEMA integral uniformity increased from 3.1 to 5.0%. NEMA differential uniformity increased from 2.4 to 3.8% and the UI increased from 1.3 to 2.6.

Extrinsic measurements showed more striking changes. When the flood phantom alone was used, absolute uniformity (Keyes method) in the CFOV decreased from 99.5 to 96.2%, a percentage decrease of 3.3%. With 5 cm of scatter and 5 cm of back scatter (5/5) the absolute uniformity fell from 97.7% to 82.8%, a loss of 15.3% (Keyes method). The UI increased

by 55% while the NEMA integral uniformity increased by 64% and differential uniformity increased by 42%. Finally, for 10 cm of scatter and 5 cm of back scatter, the Keyes uniformity decreased from an absolute value of 96.5 to 81.4%, a 15.6% loss. The percentage increase values for the Uniform-

ity Index, NEMA integral, and NEMA differential uniformity were 46, 46, and 34%, respectively.

In Fig. 2 the results of the measurements with ^{201}TI are presented. The percentage losses (Keyes method) covering the range from SYM to A30 for the intrinsic, extrinsic flood only,

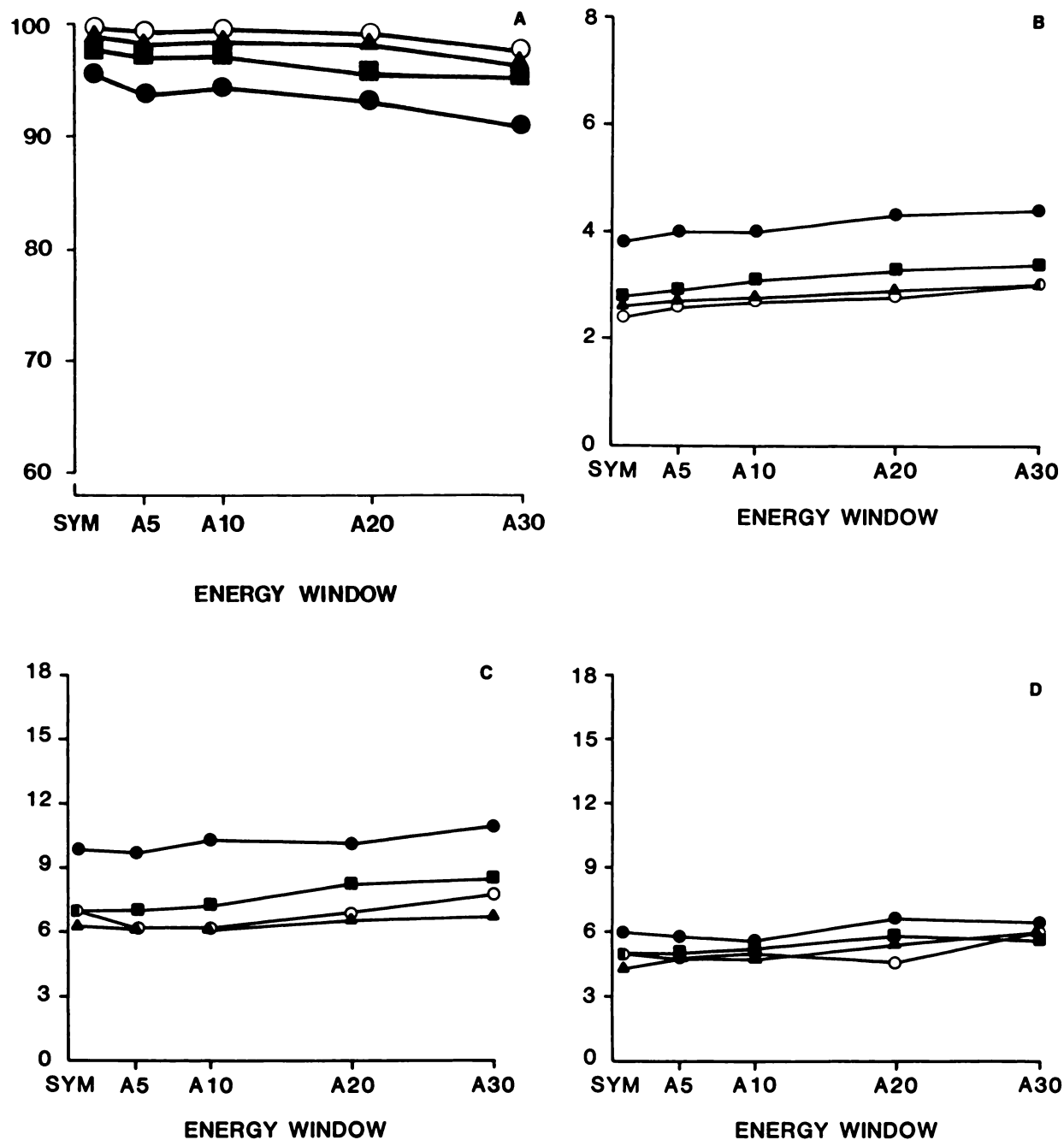


FIGURE 2

A: Thallium-201 flood field uniformity measured by percentage of cells within 5% of mean (Keyes et al.) as function of analyzer window asymmetry for four different scatter configurations: (▲) Intrinsic; (○) Extrinsic liquid-filled flood; (■) Extrinsic flood with 5 cm scatter and 5 cm backscatter; (●) Extrinsic flood with 10 cm scatter and 5 cm backscatter. B: ^{201}TI flood field uniformity measured by the UI as function of analyzer window asymmetry for four different scatter configurations. C: ^{201}TI integral flood field uniformity measured by NEMA algorithm as a function of analyzer window asymmetry for four different scatter configurations. D: ^{201}TI differential flood field uniformity measured by NEMA algorithm as function of analyzer window asymmetry for four different scatter configurations

TABLE 1
Extrinsic Count Loss for Nominal Intrinsic Window Settings

Radionuclide	^{99m} Tc		²⁰¹ Tl		¹³¹ I	
Window size	20%		25%		20%	
	Added scatter (cm)		Percent count loss relative to SYM window			
Source	Forward	Back	A05	A10	A20	A30
^{99m} Tc						
Flood	0	0	7.1	12.4	22.1	33.0
Flood	5	5	12.3	19.3	29.2	39.6
Flood	10	5	16.0	23.5	35.1	45.8
Line	5	5	13.4	21.0	31.2	41.2
Line	10	5	17.8	27.2	39.0	50.2
²⁰¹ Tl						
Flood	0	0	8.1	14.1	24.9	34.1
Flood	5	5	11.6	18.6	28.5	36.6
Flood	10	5	13.1	19.5	29.7	38.9
Line	10	5	13.1	20.0	30.8	39.4
¹³¹ I						
Flood	0	0		5.2	10.5	14.2

extrinsic 5/5, and extrinsic 10/5 configurations were -1.5, -1.6, -2.0, and -4.2%, respectively. The corresponding values for the Uniformity Index were +16, +27, +18, and +16%. NEMA integral uniformity values increased by 6, 10, 20, and 10% while NEMA differential uniformity values increased by 56, 21, 14, and 8%. Note from the graphs that the loss of uniformity was almost linear for ²⁰¹Tl as a function of window asymmetry.

The results for ¹³¹I were generally similar to those of ^{99m}Tc except that the absolute uniformity for the symmetric window was generally poorer for every test situation and the loss of uniformity as a function of window asymmetry was more rapid.

The analysis of reliability was performed with three different analysis indices: Uniformity Index, NEMA integral, and NEMA differential. For ^{99m}Tc the percentage standard deviations were 7.1, 7.4, and 7.6 for the CFOV and 10.1, 20.7, and 24.3 for the UFOV. The corresponding values for ²⁰¹Tl were 1.7, 7.4, and 2.6 (CFOV) and 2.1, 12.0, and 1.2 (UFOV).

It is important to note that the degree of asymmetry was defined relative to the symmetrical window for an intrinsic configuration. The loss of counts was considerably greater when scatter was present. Ten centimeters of scatter produced a loss of counts for ^{99m}Tc A05 and A10 windows of 16 and 26%, respectively. For ²⁰¹Tl the corresponding values were 13.1 and 19.5%. The values for all windows are presented in Table 1.

SPATIAL RESOLUTION

In the absence of scatter there was less than a 5.4% change in the FWHM or FWTM as a function of window asymmetry for both ^{99m}Tc and ²⁰¹Tl. When scatter was present, the expected improvement in spatial resolution was observed (Fig. 3). At a distance of 5 cm with 5 cm of back scatter the FWHM for ^{99m}Tc showed only a 2.0% improvement (average for 0 and 90° orientations) for the maximum degree of asymmetry used in these experiments (A30). A more significant improve-

ment of 8.4% was observed for the FWTM with the A30 setting.

In the higher scatter situation, 10 cm of distance with 5 cm back scatter (10/5), the maximum improvement in FWHM and FWTM was approximately double the values observed with the 5/5 configuration, 4.7 and 19.2%, respectively, even though the absolute values for the symmetric window were poorer (Fig. 3). Although the FWHM and FWTM values continued to improve as the analyzer window was set at greater degrees of asymmetry, most of the advantage was attained with the A10 window.

Measurements of spatial resolution changes for ²⁰¹Tl were made with only the high scatter (10/5) configuration. The absolute values of the FWHM and FWTM for ²⁰¹Tl with the SYM window were poorer than for ^{99m}Tc, 12.8 and 53.1 mm, respectively, but the percentage improvement for the A30 window was more than double the values for ^{99m}Tc, 7.4 and 18.8% respectively, for the same scatter configuration (Fig. 3). It is important to note that in contrast to ^{99m}Tc, almost the full advantage in spatial resolution improvement was found at the A05 window setting for ²⁰¹Tl. No real improvement in FWHM and FWTM values was noted beyond the A10 setting.

DISCUSSION

These experiments have served to quantitate the degree of improvement in spatial resolution and the loss of field uniformity as a function of analyzer window asymmetry for one specific camera of one manufacturer. Despite this limitation, we believe that our results can be generalized to other scintillation cameras because the underlying physical principles remain the same.

In the presence of scattering media, spatial resolution improved when asymmetric windows were used. Separate experiments demonstrated that contrast also improves (22). However, the degree to which this advantage can be utilized depends on the concomitant loss in field uniformity. This will depend on a number of factors: (a) the state of tune of the camera being used; (b) the nature of the specific energy correction circuitry employed (64 × 64 compared with 128 × 128 mapping); (c) the presence or absence of linearity (distortion) correction circuitry; and (d) the energy resolution of the detector system.

Because the camera that was used for this study did not have both energy and linearity correction circuitry, it was not surprising to observe a significant loss of field uniformity with increasing window asymmetry. It was interesting to note that for ^{99m}Tc the 5/5 and 10/5 scatter configurations gave similar curves as a function of window asymmetry while they were significantly different for ²⁰¹Tl (Figs. 1 and 2). Furthermore, ^{99m}Tc uniformity showed the largest percentage decrease with increased window asymmetry. At high degrees of asymmetry, A20 and A30, fine structure of the same spatial frequency as the correction matrix appeared in the

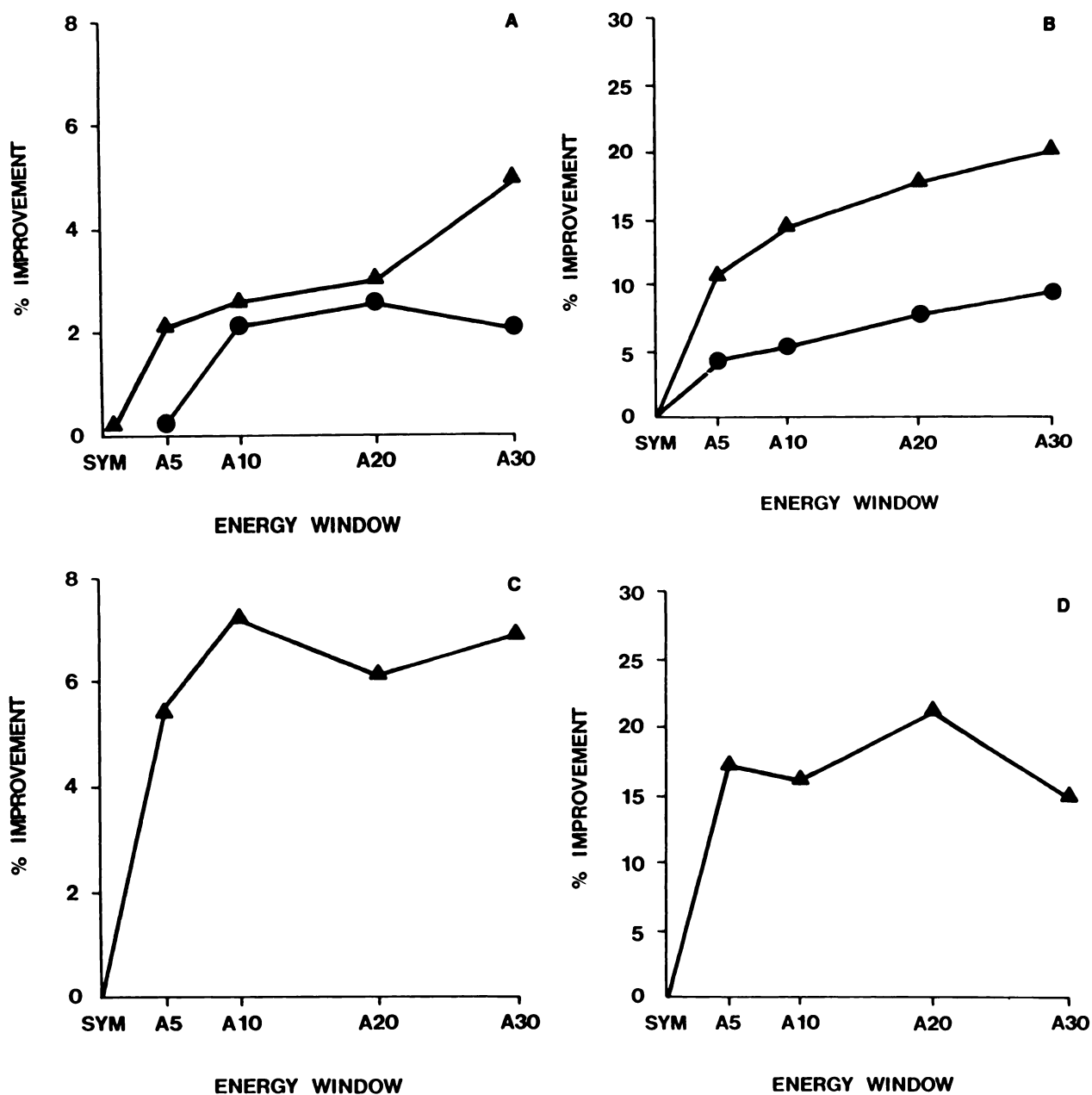


FIGURE 3

A: Percentage improvement in FWHM of extrinsic line spread function for ^{99m}Tc with two different scatter configurations. (●) 5 cm of scatter with 5 cm of backscatter; (▲) 10 cm of scatter with 5 cm of backscatter. Reference values for FWHMs are 7.50 and 11.2 mm, respectively (A, B). B: Percentage improvement in FWTM of extrinsic line spread function for ^{99m}Tc with two different scatter configurations. The reference values for the FWTMs are 15.1 and 25.6 mm, respectively. C: Percentage improvement in FWHM of extrinsic line spread function for ^{201}Tl with 10 cm of scatter and 5 cm of backscatter. Reference value for the FWHM is 12.8 mm. D: Percentage improvement in FWTM of extrinsic line spread function for ^{201}Tl with 10 cm of scatter and 5 cm of backscatter. Reference value for FWTM is 53.1 mm

images. This may be associated with the fact that as the window asymmetry increased, the relative difference between adjacent energy windows associated with the correction matrix becomes larger.

The percentage loss of uniformity with maximum asymmetry was smaller for ^{201}Tl . This may be due to the use of a wider pulse height analyzer window and the fact that the ^{201}Tl photopeak is composed of a spectrum of mercury (^{201}Hg) x-rays with energies be-

tween 66 and 80 keV. In setting the symmetric photopeak window for ^{201}Tl , the window was centered over the spectrum to obtain the maximum count rate. Therefore, the asymmetric windows represented a baseline or centerline that was advancing through a spectrum of photon energies. That situation may account for the decreased symmetric window flood field uniformity and the insensitivity of the uniformity to window asymmetry. However, it might also have been caused by the

lower energy resolution of the scintillation camera for ^{201}TI .

The poor absolute field uniformity for ^{131}I and the more rapid loss of uniformity with window asymmetry probably reflects the inability of a Tc correction map based on intrinsic conditions to correct for a markedly different energy. This may be associated with the improved energy resolution as a function of photon energy.

The four indices that were used to evaluate field uniformity provided different types of information. The methods of Keyes et al. and Cox and Diffey provide global measures of field uniformity. From the standpoint of percentage change, Cox and Diffey's technique (UI) was more sensitive. However, the Keyes method was useful in that when images were produced that displayed only the number of pixels inside the uniformity limit, visual inspection of the images provided useful information concerning the distribution of nonuniformities. The UI and the NEMA integral uniformity showed patterns of change as a function of window asymmetry that were very similar in shape although the absolute values of the UI were approximately half those of the NEMA values. According to Cox and Diffey, the UI is relatively insensitive to the number of counts per pixel once the value exceeds 100. For this reason it might be the index of choice in certain situations because fewer total image counts would be required.

In these experiments dramatic changes in differential uniformity were not observed. This is important because Cradduck et al. have shown that when differential uniformity exceeds 10% ejection fraction (EF) measurements at high EF values showed significant changes (29). This is probably due to the effect of differential uniformity on the performance of edge-finding algorithms.

On the basis of this study alone it was impossible to determine the point at which uniformity became "unacceptable" that is, caused the reader's confidence in stating that a "lesion" was present to be altered. Of course this would be markedly affected by the contrast in the "lesion." The question was addressed as a part of this study that has been reported separately. Briefly, an observer performance study demonstrated that asymmetric windows lead to increased accuracy in finding cold lesions (contrast varied from 12 to 16%) in a sea of activity. When window asymmetry of 20% or greater was used, however, the improved lesion detectability (contrast) was offset by an increased number of false positives (21).

Our results indicate that only moderate degrees of asymmetry provide nearly the maximum improvement in spatial resolution. For ^{99m}Tc , ~75% of the maximum improvement in the FWTM was found with the A10 setting in the 10/5 scatter configuration. For ^{201}TI , essentially 100% of the benefit was provided with an

A05 setting. In the presence of 10 cm of scatter these settings corresponded to a 24 and 13% loss of counts for ^{99m}Tc and ^{201}TI , respectively. It is of interest to note that the same general pattern was seen in high scatter lesion contrast measurements (22).

The rapid plateauing of FWHM and FWTM values for ^{201}TI as compared with ^{99m}Tc is difficult to explain. It may be related to the fact that the photopeak region of ^{201}TI consists of multiple x-ray photons between 66 and 80 keV. Another factor is the reduced separation between the Compton scatter peak and the photopeak. The latter suggests that asymmetric windows would be more effective for ^{201}TI , as compared with ^{99m}Tc , and this was observed at small degrees of asymmetry. The former suggests that a plateau might be observed because as the amount of scatter from one x-ray population was reduced the amount from a higher energy might be increased. Further work is needed with a monoenergetic photon emitter such as ^{201}Hg (77 keV) or xenon-133 (80 keV) and different amounts of scatter to understand this phenomenon.

CONCLUSIONS

This study verified the expected improvement in spatial resolution in high scatter situations that would be expected with the use of asymmetric windows. For the particular camera used, a loss of uniformity with increasing window asymmetry was also observed. Cameras that have been developed more recently maintain their uniformity at higher degrees of asymmetry. The fact that most of the improvement in spatial resolution and contrast is gained with relatively small degrees of asymmetry (10% for ^{99m}Tc and 5% for ^{201}TI) suggests that large degrees of asymmetry do not offer significantly greater benefits. Furthermore, highly asymmetric windows are undesirable because of the large decrease in recorded counts per unit time. Clinical studies are underway to document these conclusions.

ACKNOWLEDGMENTS

The authors acknowledge the support of Picker Corporation, Northford, CT and Beverly Hills Medical Center, Los Angeles, CA.

REFERENCES

1. Anger HO: Gamma-ray detection efficiency and image resolution in sodium iodide. *Rev Sci Instrum* 35:693–697, 1964
2. Svedberg JB: On the intrinsic resolution of a gamma camera system. *Phys Med Biol* 17:514–524, 1972
3. Atkins FB, Beck RN, Hoffer PB, et al: Dependence of optimum baseline setting on scatter fraction and detector response function. In *Medical Radionuclide Imaging*, Vol. 1, Vienna IAEA, 1977, pp 101–118
4. Beck RN, Schuh MW, Cohen TD, et al: Effects of

- scattered radiation on scintillation detector response. In *Medical Radionuclide Imaging*, Vol. 1 Vienna, IAEA, 1969, pp 595-616
5. Hoffer PB, Beck RN: Effect of minimizing scatter using Ge(Li) detectors on phantom models and patients. In *The Role of Semiconductor Detectors in the Future of Nuclear Medicine*, Hoffer PB, Beck RN, Gottschalk A, eds. New York, The Society of Nuclear Medicine, 1971, pp 131-143
 6. Eichling JO, Ter-Pogossian MM, Rhoten AL: Analysis of the scattered radiation encountered in lower energy diagnostic scanning. In *Fundamental Problems in Scanning*, Gottschalk A, Beck RN, eds. Springfield, Illinois, Charles C. Thomas, 1968, pp 238-243
 7. Beck RN, Harper PV: Criteria for evaluating radioisotope imaging systems. In *Fundamental Problems in Scanning*, Gottschalk A, Beck RN, eds. Springfield, Illinois, Charles C. Thomas, 1968, pp 348-384
 8. Price WJ: *Nuclear Radiation Detection*, Second Edition, New York, McGraw-Hill, 1958
 9. Dresser MM, Knoll GF: Results of scattering in radioisotope imaging. In *IEEE Transactions on Nuclear Science* Volume NS-20, New York, The Institute of Electrical and Electronics Engineers, Inc., 1973, pp 266-272
 10. Filipow LJ, Macey DJ, Munro TR: The measurement of the depth of a point source of a radioisotope from gamma ray spectra. *Phys Med Biol* 24:341-352, 1979
 11. Steidley JW: Imaging capabilities of germanium gamma cameras, PhD Thesis, Ohio State University, Columbus, Ohio, 1977
 12. Harris CC: Certain fundamental physical considerations in scanning. In *Scintillation Scanning in Clinical Medicine*, Quinn JL, ed. Philadelphia, W. B. Saunders Co., 1964, pp 1-13
 13. Oberley LW, Ehrhardt JC, Lensink SC: The variable baseline scanner. *Phys Med Biol* 17:630-637, 1972
 14. Sanders TP, Sanders TD, Kuhl DE: Optimizing the window of an Anger camera for Tc-99m. *J Nucl Med* 12:703-706, 1971
 15. Lange RC: A simpler method for optimizing the window of the Anger camera for Tc-99m. *J Nucl Med* 13:342, 1972
 16. Rollo FD: An index to compare the performance of scintigraphic imaging systems. *J Nucl Med* 15:757-762, 1974
 17. Bloch P, Sanders T: Reduction of the effects of scattered radiation on a sodium iodide imaging system. *J Nucl Med* 14:67-72, 1973
 18. Jansson LG, Parker RP: Pitfalls in gamma camera field uniformity correction. *Br J Radiol* 48:408-409, 1975
 19. Steidley JW, Prokop EK, Swanson SM: Regional background subtraction with asymmetrical energy window. Scientific Exhibit, 29th Annual Meeting of The Society of Nuclear Medicine, Miami, FL, 1982
 20. Lewellen T, Murano R, Weimer K, et al: The use of asymmetric windows. *J Nucl Med* 23:P30, 1982 (abstr)
 21. Lewellen T, Murano R, Weimer K, et al: The use of asymmetric windows. In *Proceedings of the Third World Congress of Nuclear Medicine and Biology*, Raynaud C, ed. Vol II, Paris, Pergamon Press, 1982, pp 1236-1239
 22. LaFontaine R, Stein MA, Graham LS: Contrast enhancement of cold lesions using asymmetric photopeak windows. *Radiol* 149P:232, 1983
 23. Collier BD, Palmer DW, Knobel J, et al: Gamma camera energy windows for Tc-99m bone scintigraphy: Effect of asymmetry on contrast resolution. *Radiol* 151:495-497, 1984
 24. Ricciardone M, Spicer KM, Frey GD, et al: Clinical comparison of Tl-201 asymmetric and symmetric energy peaking on a microprocessed energy corrected gamma camera. Scientific and Commercial Exhibits, 29th Annual Meeting of The Society of Nuclear Medicine, June 15-18, 1982, Miami Beach, Florida
 25. Graham LS: Quality Control Procedures for Field Uniformity Devices in Nuclear Medicine. U.S. Department of Health and Human Services, Food and Drug Administration, FDA 83-8154, Washington, DC, 1983
 26. Keyes JW, Gazella GR, Strange DR: Image analysis by on-line minicomputer for improved camera quality control. *J Nucl Med* 17:653, 1972
 27. Cox NJ, Diffee BL: A numerical index of gamma-camera uniformity. *Br J Radiol* 49:734, 1976
 28. Performance Measurements of Scintillation Cameras: Standards Publication/No. NU 1-1980, National Electrical Manufacturers Association, Washington, DC, 1980
 29. Cradduck TD, Busemann-Sokole E: Effects of improper camera analyzer window setting on measurement of ejection fraction using a cardiac phantom. *Med Phys* 10:549, 1983